J Mol Model (2014) 20:2493
DOI 10.1007/s00894-014-2493-0

ORIGINAL PAPER

Competition between π-hole interaction and hydrogen bond in the complexes of F_2XO (X = C and Si) and HCN

Xin Guo · Lishui Cao · Qingzhong Li · Wenzuo Li · Jianbo Cheng

Received: 13 August 2014 / Accepted: 6 October 2014 / Published online: 23 October 2014

Abstract Complexes $F_2XO\cdots HCN$ (X = C and Si) have been studied by quantum chemical calculations at the MP2/aug-cc-pVTZ level to investigate the competition between π-hole interaction and hydrogen bond. F_2XO has a dual role of a Lewis acid and base with the π-hole on the X atom and the O atom to participate in the π-hole interaction and hydrogen bond with HCN, respectively. Both types of interactions become stronger for X = Si, and the π-hole interaction is much stronger than the hydrogen bond, particularly, the π-hole interaction in $F_2SiO\cdots NCH$ complex shows a binding energy of −119.8 kJ mol^{-1}. The C-H···O hydrogen bond is dominated by the electrostatic interaction, and this conclusion holds for the π-hole interaction in $F_2CO\cdots NCH$ complex, but the electrostatic and polarization contributions are similar in $F_2SiO\cdots NCH$ complex.

Keywords Competition · Hydrogen bond · π-hole interaction

Introduction

Hydrogen bond is of great importance in chemistry and the related disciplines since it plays an important role in catalytic reactions [1], molecular materials [2], molecular recognition [3], and biological systems [4]. The strength of hydrogen bond varies in a large range from several kJ mol^{-1} to over 100 kJ mol^{-1}, and this character, together with its directionality, makes hydrogen bond have diverse applications. If the proton donor and acceptor molecules in hydrogen bonds are multifunctional, namely, more than one acid and base site, there is competition between hydrogen bond and other types of interactions [5–10]. This competition occurs not only between different types of hydrogen bonds but also between hydrogen bond and halogen bond, which is another important intermolecular interaction with a base site in Lewis bases pointing to the σ-hole (a region of positive electrostatic potential) observed on the outer surface of a covalently bonded halogen atom [11]. Hypohalous acid has often been used as a model to study the competition between hydrogen bond and halogen bond with H_2CO [12], H_2CS [13], benzene [14], formamidine [15], and some nitrogenated bases (NH_3, N_2, and HCN) [16] as the Lewis bases.

Hydrogen cyanide (HCN) is one of the most common interstellar molecules [17], produced in space from the reactions of ammonia and methane [18], and it plays a role in atmospheric chemistry as a result of its release by biomass burning [19], thus HCN has received considerable attention. HCN has a dual role of the proton donor and the acceptor in hydrogen bonds, and as the proton donor it can form different types of hydrogen bonds such as dihydrogen bonds in LiH···HCN and NaH···HCN complexes [20], single-electron hydrogen bonds in $H_3C\cdots HCN$ [21] and $H_2B\cdots HCN$ [22] complexes. Both molecules in these complexes can also form another interaction, besides the hydrogen bond, for examples, a lithium bond in HCN···LiH complex [23] and a partially covalent interaction in $HCN\cdots CH_3$ [21] and $HCN\cdots BH_2$ [22] complexes. Both types of interactions in these complexes can compete, although the hydrogen bond is weaker.

According to the distribution of electrostatic potentials on the group IV atoms, Murray, Lane and Politzer suggested that the group IV atoms can interact favorably with Lewis bases through the σ-hole found on covalently-bonded group IV atoms [24]. This σ-hole interaction [25] was recently named as tetrel bonding [26]. Mani and Arunan [27] performed a detailed theoretical analysis for the tetrel bonding in the complexes of methanol as the tetrel bond donor with the Lewis

X. Guo · L. Cao · Q. Li (✉) · W. Li · J. Cheng
The Laboratory of Theoretical and Computational Chemistry, School of Chemistry and Chemical Engineering, Yantai University, Yantai 264005, People's Republic of China
e-mail: liqingzhong1990@sina.com

bases Y = H_2O, H_2S, HF, HCl, HBr, ClF, LiF, LiCl, LiBr, NH_3, and PH_3, and the results indicated that the methyl groups adjoined with electron-withdrawing substituents can participate in the formation of tetrel bonding. The existence of tetrel bonding was further validated with experimental charge density analysis and a large number of known crystal structures exhibit structural motifs [28]. The other atoms of group IV are more favorable to form a σ-hole interaction (tetrel bonding), which is often a preliminary stage of the S_N2 reaction [29]. Such contacts were also observed in the solid-state structure of $Si(ONMe_2)_4$ and related compounds [30, 31] as well as in perhalocyclohexasilane compounds [32], thus they might serve as a new possible molecular linker [26]. This new type of σ-hole interaction has attracted our attention recently [33].

In the present paper, the complexes formed between F_2XO (X = C and Si) and HCN have been used to study the competition between π-hole interaction and hydrogen bond. Carbonyl fluoride (F_2CO) has been suggested as a chamber-cleaning agent to replace the traditional perfluorocarbons used in the plasma semiconductor industry [34], and it plays an important role in the photochemistry of the Earth's upper atmosphere [35], thus its structures and properties have been studied [36–38]. Equilibrium structure and fundamental vibrational wavenumbers of difluorosilanone (F_2SiO) have been obtained with high-level ab initio calculations [39]. Despite the potential importance of F_2CO and HCN in atmospheric chemistry, to the best of our knowledge, neither theoretical nor experimental investigations have been performed for their complexes. The present work focuses on their stabilities, electronic structures, and vibrational frequencies. The nature and formation mechanism of π-hole interaction have been compared with those of hydrogen bond.

Theoretical methods

All geometry optimization and frequency calculations were carried out via the Gaussian 09 program [40] at the MP2/aug-cc-pVTZ level of theory. All structures were confirmed to be local minima on the potential energy surface with no imaginary frequency. The interaction energies in the dyads were calculated with the formulas of $\Delta E_{AB} = E_{AB} - E_A - E_B$, where E_{AB} is the energy of the complex, while E_A and E_B are the energies of the monomers A and B with the optimized geometries. The interaction energies were corrected for basis set superposition error (BSSE) using the counterpoise procedure of Boys and Bernardi [41] and deformation energy (DE), defined as the difference in energy between the complex monomer and the optimized one.

Molecular electrostatic potentials (MEPs) at the 0.001 electrons $Bohr^{-3}$ isodensity surfaces of F_2XO were calculated with Wave Function Analysis-Surface Analysis Suite (WFA-SAS) program [42] at the MP2/aug-cc-pVTZ level. The wavefunction obtained at the MP2/aug-cc-pVTZ level was used to calculate the electron density at the critical point and plot the molecular graph using AIM2000 software [43]. To gain an insight into the nature of the investigated intermolecular interactions, the energy decomposition analysis (EDA) was performed within the GAMESS program [44] with the LMOEDA method [45] at the MP2/aug-cc-pVTZ level.

Results and discussion

Molecular electrostatic potential (MEP) has been demonstrated to be effective in predicting and analyzing noncovalent interactions. To find out the possible interaction modes involved with F_2XO, the MEP maps of F_2CO and F_2SiO monomers are plotted in Fig. 1. The most local positive and negative MEPs in F_2CO and F_2SiO are clearly observed from Fig. 1. F_2XO (X = C and Si) exhibits two regions of positive MEPs (π-holes) [46], which are perpendicular to portions of the molecular framework. The value of MEP is 1.835 eV and 3.447 eV for the π-hole in F_2CO and F_2SiO, respectively. Thus F_2XO can participate in a π-hole interaction with the π-hole as a Lewis acid, and the π-hole of F_2SiO is a stronger Lewis acid than that of F_2CO in the formation of π-hole interaction. Besides, the negative MEPs are found at the outermost region of the O, and the F atoms in F_2SiO have much smaller negative MEPs than the O atom and even the MEPs of the F atoms in F_2CO are positive with a little value. This indicates that F_2XO can act as two types of Lewis bases with the O and F atoms simultaneously and F_2SiO is a stronger Lewis base than F_2CO.

According to the MEPs of F_2XO, it can be concluded that this molecule may interact with HCN through three interaction modes: a H···O hydrogen bond between the H atom of HCN and the O atom of F_2XO, a bifurcate H···F hydrogen bond between the H atom of HCN and the two F atoms of F_2XO, and a π-hole interaction between the N atom of HCN and the π-hole of F_2XO. The three interaction modes are labeled as HB1, HB2, and PHB, respectively. Figure 2 shows the equilibrium structures of six dyads of F_2XO and HCN. Accordingly, the six dyads are denoted as C-HB1, Si-HB1, C-HB2, Si-HB2, C-PHB, and Si-PHB, respectively. The existence of these interactions can be evidenced by the presence of a bond critical point (BCP) between both molecules (a small red point in Fig. 3). The bifurcate H···F hydrogen bond is also characterized by the presence of a ring critical point (RCP, a small yellow point in Fig. 3).

Table 1 presents the binding distance and interaction energy in the dyads. The binding distance in the C-H···O hydrogen bond is smaller than the sum of the van der Waals radii of the corresponding atoms (2.72 Å for H and O atoms) [47], and Si-HB1 displays a shorter binding distance than C-HB1. A similar result is also found for the C-H···F hydrogen bond in

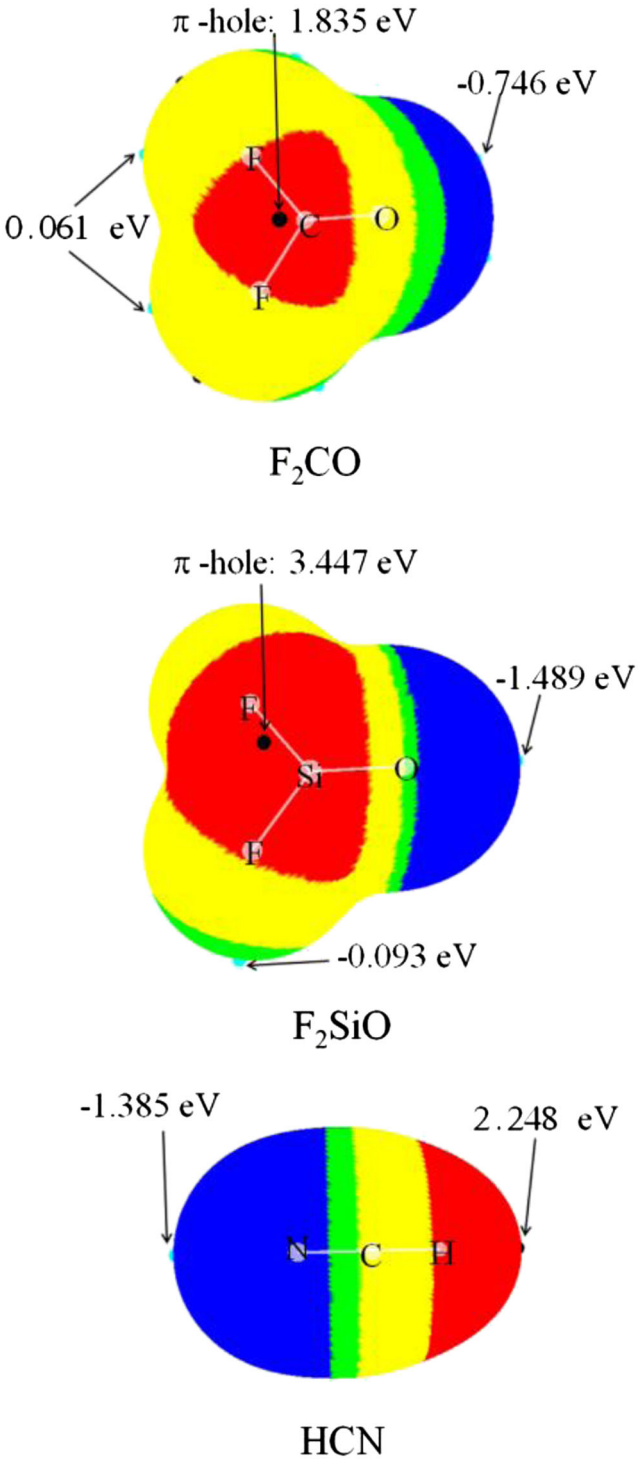

Fig. 1 Molecular electrostatic potentials of F_2XO (X = C and Si) and HCN. Color ranges are: red, greater than 0.82; yellow, between 0.82 and 0; green, between 0 and −0.27; blue, less than −0.27. All are in eV

C-HB2, however, in Si-BH2, it is larger than the sum of the van der Waals radii of the corresponding atoms (2.67 Å for H and F atoms), indicating that the C-H···F interaction is very weak and belongs to a van der Waals interaction. Si-PHB has a shorter binding distance relative to the sum of the van der

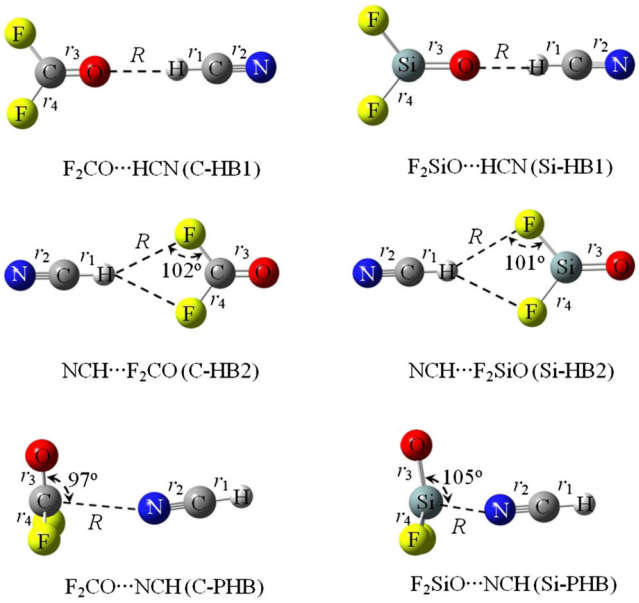

Fig. 2 Structures of π-hole interaction- and hydrogen-bonded dyads formed of F_2XO (X = C and Si) and HCN

Waals radii of the corresponding atoms (3.65 Å for Si and N atoms) than C-PHB, where the sum of the van der Waals radii of the C and N atoms is 3.25 Å.

We first consider the effect of BSSE on the interaction energy. The proportion of BSSE to the interaction energy is about 71–164 % for the van der Waals interaction, 11–20 % for the hydrogen bond, and 7–17 % for the π-hole interaction. Clearly, BSSE has a great effect on the interaction energy of weak van der Waals interaction, but its effect on the interaction energies of hydrogen bond and π-hole interaction is within acceptable range. It is necessary to point out that this van der Waals complex is not our focus in this paper. In addition, the

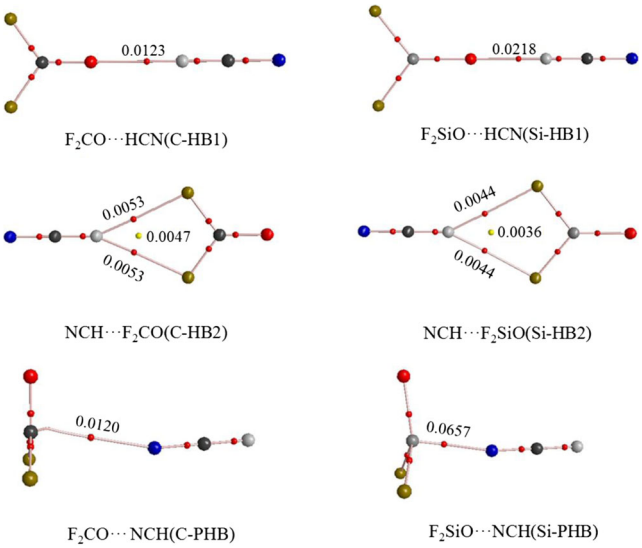

Fig. 3 Molecular graphs of dyads. Yellow and red dots indicate the locations of ring and bond critical points, respectively. Electron densities at the RCPs and BCPs are in au

Table 1 Binding distance (R, Å) and interaction energy (ΔE, kJ mol^{-1}) corrected for BSSE and DE in the dyads at the MP2/aug-cc-pVTZ level

	R	ΔE	BSSE	ΔE^{CP}	DE	ΔE^{CP+DE}
C-HB1	2.174	−13.46	2.66	−10.8	0.2	−11.0
C-HB2	2.549	−3.15	2.25	−0.9	0.13	−1.03
C-PHB	2.767	−17.22	2.92	−14.3	0.3	−14.6
Si-HB1	1.971	−28.06	3.96	−24.1	0.3	−24.4
Si-HB2	2.647	−1.39	2.29	0.9	0.4	0.5
Si-PHB	1.957	−102.97	7.47	−95.5	24.3	−119.8

$\Delta E^{CP} = \Delta E + \text{BSSE}$, $\Delta E^{CP+DE} = \Delta E + \text{BSSE} - \text{DE}$

effect of BSSE on the hydrogen bond and π-hole interaction is more prominent in the F_2CO complex than that in the F_2SiO counterpart. Then we consider the effect of deformation of the monomer on the interaction energy. One can see from Table 1 that the deformation energy is very small in most complexes except $F_2SiO\cdots NCH$, where the geometry of F_2SiO has a prominent deviation from the planar structure in the monomer. In the following discussion, the interaction energy corrected for BSSE is used in all cases unless otherwise stated.

The C-H···O hydrogen bond in Si-HB1 is stronger than that in C-HB1, which is consistent with the negative MEP on the O atom in F_2CO and F_2SiO, giving a hint that the electrostatic interaction is important in the formation of C-H···O hydrogen bond. The stronger C-H···O hydrogen bond in Si-HB1 is characterized with the larger elongation of C-H bond (0.009 Å) and the bigger red shift of C-H stretch vibration frequency (−120 cm^{-1}) (Table 2). This conclusion is further confirmed by the electron density at the H···O BCP in Fig. 3, which is 0.0123 au and 0.0218 au in C-HB1 and Si-HB1, respectively. The C-H···O hydrogen bond results in a small and similar change in the X=O, F-X, and C≡N bond lengths as well as the shift of C≡N stretch vibration frequency in C-HB1 and Si-HB1, although they have a great difference in stability. Interestingly, the C-H···O hydrogen bond in Si-HB1 is stronger than the O-H···O hydrogen bond in water dimer with the interaction energy of −5.01 kcal mol^{-1} at the CCSD(T)/CBS level [48].

Table 2 Changes of bond lengths (Δr, Å) and frequency shifts of stretch vibrations (Δv, cm^{-1}) in the dyads at the MP2/aug-cc-pVTZ level

	Δr_1	Δr_2	Δr_3	Δr_4	Δv_1	Δv_2
C-HB1	0.002	0.001	0.002	−0.006	−19	3
C-HB2	0.000	0.000	−0.003	0.004	12	1
C-PHB	0.001	−0.001	0.001	−0.001	−9	10
Si-HB1	0.009	0.000	−0.001	−0.005	−120	−1
Si-HB2	−0.001	0.000	−0.001	0.004	14	0
Si-PHB	0.003	−0.012	0.007	0.018	−20	113

The interaction in C-HB2 and Si-HB2 is very weak with the interaction energy less than −1 kJ mol^{-1}, and even the interaction energy in Si-HB2 is positive, which is inconsistent with the MEPs on the F atoms in F_2CO and F_2SiO, indicating that the electrostatic contribution is feeble in the C-H···F interaction. This weak C-H···F interaction leads to a tiny change in the C-H and C≡N bond lengths but an observed blue shift (12–14 cm^{-1}) of the C-H stretch vibration. Clearly, the C-H stretch vibration undergoes a change from a blue shift to a red shift with the increase of interaction strength. Such shift change has also been observed for the H-Ar stretch vibration in FArH···CO when it combines a lithium bond with CH_3Li [49]. The X-F bond is elongated in the C-H···F interaction, which is reverse to the contraction of this bond in the C-H···O hydrogen bond. This weak C-H···F interaction is also characterized with the small electron density at the H···F BCP and RCP, and its change in strength can also be estimated with the electron density.

As expected, the π-hole interaction in Si-PHB is much stronger than that in C-PHB, adhering to the variation of MEP on the π-hole in F_2CO and F_2SiO. However, the rangeability of the PHB interaction energy is more prominent than that of the MEP on the π-hole in F_2XO. Thus we conclude that there is another important contribution to the stability of C-PHB and Si-PHB, although the electrostatic contribution is important for it. The interaction energy corrected for BSSE and DE is about −120 kJ mol^{-1} in Si-PHB, thus the π-hole interaction in this complex is very strong. This strong π-hole interaction in Si-PHB is characterized by a big electron density at the Si N BCP, which is much larger than that at the C···N BCP in C-PHB, although both BCPs are different in nature. The weak π-hole interaction in C-PHB causes a small change in the geometry and a small shift of bond stretch vibrations, whereas the strong one in Si-PHB makes the related bonds changed greatly and the C≡N stretch vibration exhibits a large blue shift of 113 cm^{-1}, which is large enough for the triple bond.

The interaction energy in the π-hole interaction is more negative than that in the C-H···O hydrogen bond, that is, the π-hole interaction is stronger than the C-H···O hydrogen bond. Their difference in strength is small for the F_2CO complex, showing both types of interactions can compete between F_2CO and HCN. However, this difference is very large in the F_2SiO complex, indicating the π-hole interaction is dominant when F_2SiO interacts with HCN, although the C-H···O hydrogen bond can also not be neglected. The above conclusions can be rationalized with the difference in electrostatic potential between the Lewis acid and base. For the complexes of F_2CO and HCN, this difference is close for both the π-hole interaction and C-H···O hydrogen bond. However, for the complexes of F_2SiO and HCN, it is obviously larger in the π-hole interaction than that in the C-H···O hydrogen bond.

To probe into the feature of electron density shifts during the formation of the complex, the maps of electron density difference in the dyads are presented in Fig. 4. These maps were obtained by subtracting the electron density of each isolated molecule fixed with the geometry in the dyad from the total electron density of the dyad. Red areas indicate an increased electron density, whereas blue regions represent a decreased electron density. For the three different types of interactions, there are some common features in the electron density shifts: the concentrated density occurs for the electron donor atoms, while the loosened density is observed for the electron acceptor atoms. Both types of areas become larger in the same order of HB2<HB1<PHB and F_2CO<F_2SiO as the change of the interaction energy in these dyads. The electron density shifts can be effective to compare the strength of C-H···F interaction in C-HB2 and Si-HB2 although this interaction is very weak. The red region on the O atom in HB1 is closer to the blue one on the H atom with the enhancement of C-H···O hydrogen bond. For Si-PHB with a strong π-hole interaction, the red region on the N atom has been enwrapped by the blue region from the π-hole. Additionally, the electron densities on the F atoms in HB1 have reverse shifts to those in PHB.

To unveil the nature of the above three types of interactions, the interaction energies in the dyads formed of F_2XO and HCN were decomposed into five components: electrostatic energy (E^{ele}), exchange energy (E^{ex}), repulsion energy (E^{rep}), polarization energy (E^{pol}), and dispersion energy (E^{disp}), and the results are collected in Table 3. For the C-H···O hydrogen bond in C-HB1 and Si-HB1, the attractive terms become larger in order of $E^{ele} > E^{ex} > E^{pol} > E^{disp}$, although the E^{disp} term is positive in Si-HB1, indicative of the electrostatic nature of hydrogen bonds with moderate strength like O-H···O hydrogen bond in water dimer [45]. For the weak C-H···F interaction in C-HB2 and Si-HB2, the E^{ele} term is even positive and the E^{disp} term is more negative than the E^{pol} one, which is consistent with the nature of weak interactions [50]. For the π-hole interaction in C-PHB and Si-PHB, the very large E^{ex} and E^{rep} indicate that there is a significant orbital overlap between F_2XO and HCN. The electrostatic energy is also dominant in the π-hole interaction of C-PHB like that in the C-H···O hydrogen bond, although the E^{pol} and E^{disp} terms have a different change for both types of interactions. The π-hole interaction in Si-PHB shows a relatively large value of E^{pol} = −202.5 kJ mol^{-1}, although it is a little smaller than the E^{ele} value, suggesting that the orbitals undergo significant change in their shapes, which is a typical feature in the formation of a covalent bond and can be reflected in the deformation of F_2SiO in the complex. Thus the E^{pol} term has a comparable contribution to the stability of Si-PHB with the E^{ele} term.

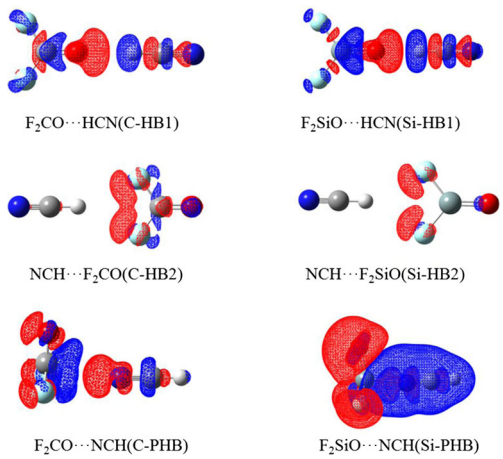

Fig. 4 Electron density shifts in the dyads. Red regions indicate increased density and blue regions indicate decreased density. Contours are shown at the 0.0005 au level

Table 3 Energy components (E, kJ mol^{-1}) and interaction energy (ΔE, kJ mol^{-1}) in the dyads at the MP2/aug-cc-pVTZ level

	E^{ele}	E^{ex}	E^{rep}	E^{pol}	E^{disp}	ΔE^{int}
C-HB1	−16.2	−12.2	22.2	−4.1	−0.8	−11.1
C-HB2	1.3	−4.8	8.6	−1.5	−4.7	−1.1
C-PHB	−22.8	−25.9	46.4	−4.8	−7.6	−14.7
Si-HB1	−41.4	−32.4	58.9	−12.1	2.5	−24.5
Si-HB2	3.3	−3.8	6.7	−1.3	−4.4	0.5
Si-PHB	−240.7	−292.8	606.5	−202.5	6.9	−122.6

Conclusions

Binary systems composed of F_2XO (X = C and Si) and HCN molecules have been investigated. Both molecules can be combined with a C-H···O hydrogen bond, a C-H···F van der Waals interaction, and a π-hole interaction, respectively. The C-H···O hydrogen bond can compete with the π-hole interaction in the complexes of F_2CO and HCN, while F_2SiO is more inclined to form the π-hole interaction than the C-H···O hydrogen bond with HCN. Both C-H···O hydrogen bond and π-hole interaction are stronger in the F_2SiO complexes than those in the F_2CO counterpart. The C-H···F van der Waals interaction is dominated by dispersion energy, while the C-H···O hydrogen bond is governed by electrostatic interaction. The π-hole interaction in F_2CO···NCH complex exhibits an electrostatic nature, while that in F_2SiO···NCH complex is controlled jointly by electrostatic and polarization energies. For F_2SiO···NCH complex, the large polarization energy in the π-hole interaction indicates that this bond has a nature of partially covalent interaction.

Acknowledgments This work was supported by the Outstanding Youth Natural Science Foundation of Shandong Province (JQ201006)

and the Program for New Century Excellent Talents in University (NCET-2010-0923).

References

1. Schowen KB, Limbach HH, Denisov GS, Schowen RL (2000) Biochim Biophys Acta 1458:43–62
2. Schulze BM, Shewmon NT, Zhang J, Watkins DL, Mudrick JP, Cao W, Zerdan RB, Quartararo AJ, Ghiviriga I, Xue J, Castellano RK (2014) J Mater Chem A 2:1541–1549
3. Tóth G, Bowers SG, Truong AP, Probst G (2007) Curr Pharm Des 13:3476–3493
4. Głowacki ED, Irimia-Vladu M, Bauer S, Sariciftci NS (2013) J Mater Chem B 1:3742–3753
5. Sears WA, Hudolin ML, Jenkins HA, Mawhinney RC, Mackinnon CD (2008) J Coord Chem 61:825–835
6. Burrows AD, Kelly DJ, Mohideen MIH, Mahon MF, Pop VM, Richardson C (2011) CrystEngComm 13:1676–1682
7. Schmies M, Patzer A, Fujii M, Dopfer O (2011) Phys Chem Chem Phys 13:13926–13941
8. Jones RH, Knight KS, Marshall WG, Coles SJ, Horton PN, Pitak MB (2013) CrystEngComm 15:8572–8577
9. Bhattacharya S, Jana A, Mohanta S (2013) CrystEngComm 15: 10374–10382
10. Singh SK, Kumar S, Das A (2014) Phys Chem Chem Phys 16:8819–8827
11. Politzer P, Murray JS, Clark T (2010) Phys Chem Chem Phys 12: 7748–7757
12. Li QZ, Xu XS, Liu T, Jing B, Li WZ, Cheng JB, Gong BA, Sun JZ (2010) Phys Chem Chem Phys 12:6837–6843
13. Li QZ, Jing B, Li R, Liu ZB, Li WZ, Luan F, Cheng JB, Gong BA, Sun JZ (2011) Phys Chem Chem Phys 13:2266–2271
14. Zhao Q, Feng D, Sun Y, Hao J, Cai Z (2011) J Mol Model 17:1935–1939
15. An XL, Zhuo HY, Wang YY, Li QZ (2013) J Mol Model 19:4529–4535
16. Alkorta I, Blanco F, Solimannejad M, Elguero J (2008) J Phys Chem A 112:10856–10863
17. Herbst E, van Dishoeck EF (2009) Annu Rev Astron Astrophys 47: 427–480
18. Matthews CN, Minard RD (2006) Faraday Discuss 133:393–401
19. Li QB, Jacob DJ, Yantosca RM, Heald CL, Singh HB, Koike M, Zhao Y, Sachse GW, Streets DG (2003) J Geophys Res 108:8827, 48/1–48/43
20. Alkorta I, Elguero J, Moo O, Yanez M, Del Bene JE (2002) J Phys Chem A 106:9325–9330
21. Solimannejad M, Alikhani ME (2005) Chem Phys Lett 406:351–354
22. Wang WJ, Li QZ (2011) Comput Theor Chem 977:128–133
23. Li QZ, Hu T, An XL, Li WZ, Cheng JB, Gong BA, Sun JZ (2009) ChemPhysChem 10:3310–3315
24. Murray JS, Lane P, Politzer P (2009) J Mol Model 15:723–729
25. Politzer P, Murray JS, Clark T (2013) Phys Chem Chem Phys 15: 11178–11189
26. Bauza A, Mooibroek TJ, Frontera A (2013) Angew Chem Int Ed 52: 12317–12321
27. Mani D, Arunan E (2013) Phys Chem Chem Phys 15:14377–14383
28. Thomas SP, Pavan MS, Row TNG (2014) Chem Commun 50:49–51
29. Grabowski SJ (2014) Phys Chem Chem Phys 16:1824–1834
30. Mitzel NW, Losehand U (1997) Angew Chem Int Ed 36:2807–2809
31. Mitzel NW, Blake AJ, Rankin DWH (1997) J Am Chem Soc 119: 4143–4148
32. Choi SB, Kim BK, Boudjouk P, Grier DG (2001) J Am Chem Soc 123:8117–8118
33. Li QZ, Guo X, Yang X, Li WZ, Cheng JB, Li HB (2014) Phys Chem Chem Phys 16:11617–11625
34. Mitsui Y, Ohira Y, Yonemura T, Takaichi T, Sekiya A, Beppu T (2004) J Electrochem Soc 151:G297–G301
35. Rinsland CP, Zander R, Brown LR, Farmer CB, Park JH, Norton RH III, Russell JM, Raper OF (1986) Geophys Res Lett 13:769–772
36. Kato H, Nunes Y, Duflot D, Limao-Vieira P, Tanaka H (2011) J Phys Chem A 115:2708–2718
37. Faria SHDM, da Silva Jr JV, Haiduke RLA, Vidal LN, Vazquez PAM, Bruns RE (2007) J Phys Chem A 111:7870–7875
38. Hoshino M, Limão-Vieira P, Probst M, Nunes Y, Tanaka H (2011) Int J Mass Spectrom 303:125–128
39. Breidung J, Thiel W (2000) Z Anorg Allg Chem 626:362–367
40. Frisch MJ, Trucks GW, Schlegel HB, Scuseria GE, Robb MA, Cheeseman JR, Montgomery JA Jr, Vreven T, Kudin KN, Burant JC, Millam JM, Iyengar SS, Tomasi J, Barone V, Mennucci B, Scalmani G, Cossi M, Rega N, Petersson GA, Nakatsuji H, Hada M, Ehara M, Toyota K, Fukuda R, Hasegawa J, Ishida M, Nakajima T, Honda Y, Kitao O, Nakai H, Klene MLX, Knox JE, Hratchian HP, Cross JB, Adamo C, Jaramillo J, Gomperts R, Stratmann RE, Yazyev O, Austin AJ, Cammi R, Pomelli C, Ochterski JW, Ayala PY, Morokuma K, Voth GA, Salvador P, Dannenberg JJ, ZakrzewskiVG DS, Daniels AD, Strain MC, Farkas O, Malick DK, Rabuck AD, Raghavachari K, Foresman JB, Ortiz JV, Cui Q, Baboul AG, Clifford S, Cioslowski J, Stefanov BB, Liu G, Liashenko A, Piskorz P, Komaromi I, Martin RL, Fox DJ, Keith T, Al-Laham MA, Peng CY, Nanayakkara A, Challacombe M, Gill PMW, Johnson B, Chen W, Gonzalez C, Wong MW, Pittsburgh PA, Pople JA (2009) Gaussian 09, revision A02. Gaussian Inc, Wallingford
41. Boys SF, Bernardi F (1970) Mol Phys 19:553–566
42. Bulat FA, Toro-Labbé A, Brinck T, Murray JS, Politzer P (2010) J Mol Model 16:1679–1691
43. Bader RFW (2000) AIM2000 program, v 20. McMaster University, Hamilton
44. Schmidt MW, Baldridge KK, Boalz JA, Elbert ST, Gorden MS, Jensen JH, Koseki S, Matsunaga N, Nguyen KA, Su SJ, Windus TL, Dupuis M, Montgomery JA (1993) J Comput Chem 14:1347–1363
45. Su PF, Li H (2009) J Chem Phys 131:014102
46. Murray JS, Lane P, Clark T, Riley K, Politzer P (2012) J Mol Model 18:541–548
47. Bondi A (1964) J Phys Chem 68:441–451
48. Klopper W, van Duijneveldt-van de Rijdt JGCM, van Duijneveldt FB (2000) Phys Chem Chem Phys 2:2227–2234
49. Liu XF, Li QZ, Cheng JB, Li WZ (2013) Mol Phys 111:497–504
50. Tsuzuki S, Honda K, Uchimaru T, Mikami M, Fujii A (2006) J Phys Chem A 110:10163–10168